KFKI-1992-29/D
PREPRINT

Z. DONKÓ,
M. JÁNOSSY

MODELING THE CATHODE REGION OF NOBLE GAS MIXTURE DISCHARGES USING MONTE CARLO SIMULATION

Hungarian Academy of Sciences
CENTRAL
RESEARCH
INSTITUTE FOR
PHYSICS

B U D A P E S T

KFKI-1992-29/D
PREPRINT

Modeling the cathode region of noble gas mixture discharges using Monte Carlo simulation

Z. Donkó and M. Jánossy
Central Research Institute for Physics
Research Institute for Solid State Physics
H-1525 Budapest 114, P.O.B. 49, HUNGARY

Published in a short form in
Journal of Physics D: Applied Physics
Vol 25, pp 1323-1329 (1992)

HU ISSN 0368 5330

Z. Donkó and M. Jánossy: Modeling the cathode region of noble gas mixture discharges using Monte Carlo simulation KFKI-1992-29/D

ABSTRACT

A model of the cathode dark space of DC glow discharges was developed in order to study the effects caused by mixing small amounts ($\leq$ 2%) of other noble gases (Ne, Ar, Kr and Xe) to He. The motion of charged particles was described by Monte Carlo simulation. Several discharge parameters (electron and ion energy distribution functions, electron and ion current densities, reduced ionization coefficients, and current density-voltage characteristics) were obtained. Small amounts of admixtures were found to modify significantly the discharge parameters. Current density—voltage characteristics obtained from the model showed good agreement with our experimental data.

Z. Donkó and M. Jánossy: Modeling the cathode region of noble gas mixture discharges using Monte Carlo simulation KFKI-1992-29/D

KIVONAT

A ködfénykisülések katód környéki térrészének leírására kidolgozott modellünkkel vizsgáltuk kis mennyiségű adalékgázok hatását a gázkisülés jellemzőire. A számításokat He buffergázra végeztük el, az adalékgázok Ne, Ar, Kr és Xe voltak, maximálisan 2%-os koncentrációban. A töltött részecskék (elektronok és ionok) mozgásának leírására Monte Carlo szimulációt alkalmaztunk. A modell segítségével a gázkisülés számos jellemzőjét határoztuk meg (elektronok és ionok energia-eloszlása, elektron- és ionáramsűrűségek, redukált ionizációs együttható, áramsűrűség - feszültség karakterisztika). Megállapítottuk, hogy a kis mennyiségű adalékgázok jelentős mértékben befolyásolják a kisülés jellemzőit. A számítások során kapott áramsűrűség-feszültség karakterisztikák jó egyezést mutatnak a kísérleti eredményeinkkel.

1. INTRODUCTION

The cathode region of glow discharges has been the scope of both theoretical and practical interest (Den Hartog *et al* 1988, Sommerer and Lawler 1988, Carman 1989, Shi *et al* 1989). Some applications of the cathode region of the discharge are spectral lamps (Walsh 1955), hollow cathode lasers (Solanki *et al* 1979, Rózsa and Jánossy 1983) and plasma processing (Chen *et al* 1988). The theoretical interest of the cathode region arises from its important role in the maintenance of the discharge and the non-hydrodynamic properties of this region.

Hydrodynamic (or local field equilibrium) regions are usually defined as where the electron energy distribution function (EEDF) at any place depends only on the local value of the reduced field E/n (electric field to gas density ratio) (Pitchford *et al* 1990). Under local field equilibrium conditions the transport properties of charged particles, as well as the rate coefficients of different elementary processes are also functions of the local E/n. Measurements of transport and Townsend ionization coefficients are usually carried out in such environments where special care is taken to find hydrodynamic conditions. Therefore the data obtained in these experiments may not be directly applied to modeling non-hydrodynamic regions.

In the cathode dark space (CDS) of glow discharges there are very high electric field gradients. As a consequence of this the electric field changes considerably along the mean free path of the electrons. The velocity of an electron at any position is *not determined exclusively by the local value of the electric field rather by the electric field distribution along the path of the electron.* Because of this the CDS shall be considered as a non-hydrodynamic region.

There are a few basic possibilities to obtain the EEDF in the plasma. The most often used of them are the solution of Boltzmann's kinetic equation (analytically or numerically) and

the Monte Carlo (MC) type simulation of the charged particles' motion. Both of these basic approaches have their advantages and limitations, which are not discussed here and may be found elsewhere (e.g. Marode and Boeuf 1983, Graves and Surendra 1990).

The Monte Carlo simulation providing a flexible description of the particles' motion and different collision processes have been applied by several authors (Tran Ngoc An *et al* 1977, Boeuf and Marode 1982, Ohuchi and Kubota 1983, Hashiguchi and Hasikuni 1988, Yumoto *et al* 1991, Hashiguchi 1991, Jianfen Liu and Govinda Raju 1992, Date *et al* 1992). We have chosen this method for our modeling of the CDS in noble gas mixtures.

The large effects of impurities and small amounts of admixtures in gas discharges are widely known since the investigations of Kruithof and Penning (1937). In the case of glow discharges the changes of different discharge parameters (e.g. minimal maintaining potential, voltage - current characteristics) were recognized by several investigators, as well (see e.g. Weston 1968).

Measuring current density-voltage [$j(V)$] characteristics of the cathode region in noble gas mixture discharges we have found that small amounts of other noble gases admixed to He cause remarkable and admixture-specific changes of the $j(V)$ characteristics (Donkó *et al* 1991). The observed changes of the $j(V)$ characteristics in the cathode region deviate from those in the positive column of discharges, where all the other noble gases admixed to He result in an increase of the current density at constant voltage (see e.g. Willett 1974).

Although there is an increasing interest in the cathode region of the glow discharges, little effort has been made so far to model this region in noble gas mixture discharges and calculate current density-voltage characteristics.

2. THE MODEL OF THE CATHODE DARK SPACE

In this section the details of our model of the CDS are presented. First the basic features of the model are summarized (§ 2.1) then further details are given about the maintenance of the discharge and the elementary processes considered in the model (§§ 2.1.1, 2.1.2). The Monte Carlo procedure, the treatment of charged particles, the simulation process and the determination of the discharge parameters are discussed in §§ 2.2-2.7.

2.1. Formulation of the model

Our model of the CDS was developed with low current density ($j \approx$ mA/cm^2) abnormal glow discharges in mind. At low current densities thermal effects and cathode sputtering may be neglected and the low current density results low electron density in the CDS. The discharge is supposed to be stationary and driven by a DC voltage source.

The considered elementary processes include electron emission from the cathode (only due to positive ion bombardment, see § 2.1.1), elastic and inelastic (excitation and ionization) collisions of electrons with gas atoms, Penning ionization, as well as symmetric and asymmetric charge transfer processes.

The electrodes of the discharge are assumed to be plane and parallel. The edge effects are ignored in the simulation of electron motion (the electrodes are supposed to be infinite). On the other hand the discharge volume is considered to be finite when the contribution of Penning ionization is calculated. Furthermore it is supposed that the space between the two electrodes is filled entirely by the cathode dark space (CDS) and the negative glow (NG) as it is indicated in figure 1.

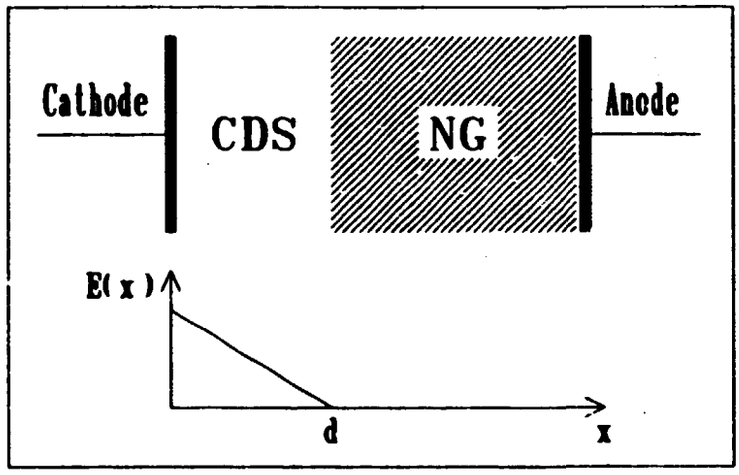

Figure 1.

The cathode region and the electric field distribution. (CDS: cathode dark space, NG: negative glow, d: length of the CDS)

The electric field distribution was chosen in accordance with experimental investigations as given by (Warren 1955, Shi *et al* 1989):

$$E(x) = (2V/d)(1-x/d), \qquad (1)$$

where V is the cathode fall voltage and d is the length of the CDS and x is the distance from the cathode.

The negative glow is considered to be a field free region and in this case the potential difference between the electrodes is equal to the cathode fall voltage V.

This model of the CDS is not a "self-consistent field" model. The electric field distribution obtained from the model is, however, as it will be shown later, very similar to the *a priori* specified field (1).

2.1.1. The maintenance of the discharge

The glow discharge is maintained by electrons ejected from the cathode due to the impact of positive ions, metastable atoms and UV photons on its surface. There are no extensive data

available for the participation of these processes in the maintenance of the discharge. Measurements of Molnar (1951) have shown that the secondary electron emission coefficients for positive ions and metastable atoms are nearly equal. The number of metastable atoms arriving at the cathode surface, however, is less than the number of positive ions because the ionization rate is expectedly about an order of magnitude greater than the metastable production rate. Furthermore the metastables diffuse in every direction, the motion of positive ions is directed towards the cathode. Investigations on the role of UV photons indicated that only a few percent of the electron current at the cathode is induced by UV photons (Helm 1979). Consequently the positive ion impact is accepted as the dominant process responsible for electron emission from the cathode.

Recent investigations have shown that most of the electron emission at the cathode is caused by positive ions created in the cathode dark space i.e. the number of positive ions entering the CDS from the negative glow is negligible (Doughty *et al* 1987, Den Hartog *et al* 1988).

If the length of the CDS (d) is known from experiments the Monte Carlo simulation can be carried out in a straightforward way. Then the results of the simulation may provide information about the different secondary processes at the cathode. To our knowledge there is no available experimental data for d in noble gas mixture discharges. However, if we assume that no ions enter the CDS from the NG, d can be obtained from our model (see § 2.7).

2.1.2. Elementary processes

The elementary processes considered in our model of the CDS are listed below (the admixed gas in denoted by X):

- Electron emission from the cathode due to positive ion impact;
- Anisotropic elastic scattering of electrons from He and X atoms;

- Electronic excitation of He and X atoms;
- Electron impact ionization:

$$He + e^- \rightarrow He^+ + 2\ e^-, \qquad (2)$$

$$X + e^- \rightarrow X^+ + 2\ e^- \qquad (3)$$

- if the admixed gas X has a lower ionization potential than the energy of He metastable levels (X=Ar,Kr,Xe), the Penning ionization:

$$He^m + X \rightarrow X^+ + He + e^-, \qquad (4)$$

where He^m denotes helium metastables;
- Charge transfer processes, namely the symmetric processes involving ions and atoms of the same type:

$$He^+ + He \rightarrow He + He^+,$$

$$X^+ + X \rightarrow X + X^+$$

and the asymmetric process:

$$He^+ + X \rightarrow He + X^+$$

Since the opposite asymmetric charge transfer process is strongly endoergic we have not taken it into account.

After summarizing the applied Monte Carlo procedure in the next section, the above processes will be discussed in more detail in §§ 2.3-2.5.

2.2. The Monte Carlo procedure

The Monte Carlo (MC) procedure applied in our model was developed for tracing the motion of electrons in non-uniform electric fields (Boeuf and Marode 1982). This method was used in our model for tracing both electrons and ions in the CDS. Only the main points of the mathematical part of the Monte Carlo

procedure are discussed here, the interested reader may find every detail in the paper of Boeuf and Marode (1982).

Although the electric field is one dimensional (1), the radial motion of the particles and their angular scattering in collision processes may be considered, providing a quite realistic description of the particles' motion. The energy dependence of the cross section of individual processes are also included.

Let us consider a particle moving along a curvilinear abscissa s. The probability of that the next collision of the particle occurs beyond s is given by:

$$P(s) = exp\left\{-\int_{s_0}^{s} Q(s)\ ds\right\}, \tag{5}$$

where s_0 is the position of the last collision and Q in a gas mixture is given by:

$$Q[\varepsilon(s)] = \sum_i (n \cdot \sigma[\varepsilon(s)])_i, \tag{6}$$

i.e. the cross sections of all the possible collision processes (σ) are weighted by the concentration of "target" atoms (n) and are summarized.

The position of the next collision (s_c) may be determined by the solution of the following equation:

$$\int_{s_0}^{s_c} Q[\varepsilon(s)]\ ds = -\ Ln(1-R_{01}), \tag{7}$$

where R_{01} is a random number uniformly distributed on the [0,1) interval. This equation is solved by Boeuf and Marode rather for the ε_c kinetic energy of the electron just before the next collision and once ε_c is known, s_c is calculated based on the conservation of energy.

The computational speed may be increased significantly if the need for numerical integration in the solution of (7) can be

eliminated. This can be done by the introduction of a so-called null-collision process (Skullerud 1968, Boeuf and Marode 1982). In this case eq. (7) is solved using the following cross section:

$$Q'(\varepsilon) = Q(\varepsilon) + Q_{NULL}(\varepsilon), \qquad (8)$$

where $Q_{NULL}(\varepsilon)$ is the cross section of the null-collision process and it is chosen in that way to result that $Q'(\varepsilon)$ remains constant within certain intervals in the CDS. The introduction of the fictive null-collision process results somewhat higher number of collisions but these additional collisions (the null-collisions) do not influence the "real" path of the particle.

The type of the collisions in the MC scheme is determined randomly. When a collision occurs, the [0,1) interval is divided into subintervals according to the cross sections of the individual elementary processes (including the null-collisions process). The actual process is chosen by the interval into which a R_{01} random number falls.

2.3. The treatment of electrons

The motion of the electrons through the CDS is traced in three dimensions by the Monte Carlo procedure described in § 2.2. In the following subsections we discuss the initial energy distribution of the electrons emitted by the cathode and the collision processes involving electrons.

2.3.1. Energy distribution of electrons emitted from the cathode

The initial kinetic energy of electrons ejected from the cathode due to positive ion impact has an upper limit $\varepsilon_{max}=E_i-2\cdot\varphi$, where E_i is the ionization potential of the gas

atom and φ is the work function of the cathode material (Hagstrum 1956). In the Monte Carlo simulation a random initial energy may be assigned to each individual electron being emitted by the cathode. In the model a uniform probability distribution is used, the ε_0 initial energy of the emitted electron is calculated by:

$$\varepsilon_0 = (E_i - 2\cdot\varphi)\cdot R_{01}, \tag{9}$$

where R_{01} is a random number uniformly distributed on the [0,1) interval. In pure He discharge E_i is the ionization potential of He, in He+X gas mixture E_i is chosen randomly for single electrons to be equal either to the ionization potential of He or that of X, as both He^+ and X^+ ions liberate electrons from the cathode.

2.3.2. Collision processes involving electrons

In the collision processes the direction (and the magnitude) of the velocity of the electron is changed except in the null-collision process when the electron proceeds without any change in its velocity. In the following we discuss the collision processes involving electron impact: the elastic scattering, excitation and the electron impact ionization. We note that the value of Q to be used in the MC procedure (equation (6)) is:

$$Q = \sum_{i=He,\,X} n_i(\sigma_{i,ela} + \sigma_{i,exc} + \sigma_{i,ion}). \tag{10}$$

The cross sections of the (elastic σ_{ela}, excitation σ_{exc} and ionization σ_{ion}) collision processes are taken from de Heer and Jansen (1977) and de Heer *et al* (1979).

The elastic scattering of electrons is nearly isotropic at low values of ε kinetic energy, while it is strongly peaked in the forward direction at high values of ε. This property of the elastic scattering is included in the model by using the

following formula for the differential cross section of elastic scattering (Boeuf and Marode 1982):

$$\sigma_{ela}(\varepsilon,\varkappa) = A \exp\{-B\sqrt{\varepsilon}\,\sin(\varkappa/2)\}, \qquad (11)$$

where $\varkappa$ is the scattering angle, the constants A and B are specific for each noble gas. The new direction of the velocity of the scattered electron is determined randomly according to (11). The coefficients A and B were determined by fitting the integral of the above formula to the total elastic cross section data. The energy loss of electrons during elastic collisions with gas atoms is neglected.

In the case of electronic excitation no energy levels are distinguished in the atom, the energy lost by the electron is randomly chosen according to the following relation:

$$-\Delta\varepsilon = \varepsilon_1 + (\varepsilon_2-\varepsilon_1)R_{01}, \qquad (12)$$

where ε_1 is the energy of the lowest excited state of the atom, and $\varepsilon_2 = \min(E_i,\varepsilon_c)$, E_i and ε_c being the ionization potential of the atom and the kinetic energy of the electron before the collision. After the collision the electron is scattered isotropically, the direction of its velocity is chosen randomly. In the model all the excited states of He are supposed to decay to the metastable levels. (We believe that the radiation trapping between the 2^1P state and the ground state of helium makes our assumption realistic.)

In electron impact ionization the scattered and the ejected electrons share randomly the remaining kinetic energy after ionization. Furthermore their velocities are assumed to be coplanar and perpendicular (Boeuf and Marode 1982).

2.4. Penning ionization

The contribution of Penning ionization in the case of He+X mixtures can be approximated by considering the diffusion of He^m

metastables out of the discharge volume. The CDS is supposed to be cylindrical having the same radius as the electrodes.

If the metastable concentration at an initial time $t=0$ is $n_m(0)$, the concentration at a time $t>0$ is given by (see e.g. Willett 1974):

$$n_m(t) = n_m(0) \cdot exp\ \{-D \cdot t/\Lambda^2\} \qquad (13)$$

where D is the diffusion coefficient of He^m metastables in He at the given He pressure and Λ is the characteristic diffusion length of He^m atoms given by:

$$\Lambda^{-2} = (\pi/d)^2 + (z_0/2r)^2 \qquad (14)$$

where d and r are the length and the radius of the cylinder and $z_0 \cong 2.405$ is the smallest root of the $J_0(z)=0$ equation, where J_0 is the zero order Bessel function of the first kind.

Applying (13) to a single metastable atom the probability of that atom being still in the CDS at a time t after its creation at $t=0$ may be given:

$$P_m(t) = exp\ \{-D \cdot t/\Lambda^2\}. \qquad (15)$$

The metastable atoms move with an average thermal velocity $\bar{v}$ and the average distance they pass through during t is $\bar{v} \cdot t$. If the Penning ionization process has a cross section σ_p then the mean free path (λ_p) of a He^m atom is given by:

$$\lambda_p = 1/(n_x \sigma_p), \qquad (16)$$

where n_x denotes the atom concentration of the gas X. The average time a He^m metastable atom needs to produce an X^+ ion can be expressed using (16):

$$\bar{t} = \lambda_p / \bar{v} = 1/(n_x \sigma_p \bar{v}). \qquad (17)$$

Substituting $\bar{t}$ into (15) the probability that the Penning reaction happens within the CDS is:

$$P_m = exp\ \{-D/(\lambda^2 n_x \sigma_p \bar{v})\} \qquad (18)$$

If an excitation process of He occurs in the simulation then a random number R_{01} is generated and a Penning ionization process is supposed to take place in the CDS if $R_{01}<P_m$, where P_m is calculated as given by (18). The cross sections of Penning ionization are taken from Muschlitz and Scholette (1960).

2.5. The treatment of ions

As a result of the high *E/n* present in most of the CDS the angular distribution of the ion velocity distribution is strongly peaked toward the cathode. The motion of positive ions is therefore treated one dimensionally (Lawler 1985, Den Hartog *et al* 1988).

The motion of the ions is basically determined by charge transfer processes. In pure He glow discharge the mean free path associated with the

$$He + He^+ \rightarrow He^+ + He \qquad (19)$$

symmetric charge transfer process is much shorter than the length of the CDS. In the case of gas mixtures additional charge transfer processes take place:

$$X + X^+ \rightarrow X^+ + X, \qquad (20)$$

$$He^+ + X \rightarrow He + X^+, \qquad (21)$$

which have a mean free path comparable to or greater than the length of the CDS. (Note that in our investigations the concentration of the admixture X is 2-3 orders of magnitude less than the concentration of He.)
This requires Monte Carlo treatment of the ions.

Since the He^+ ions can exchange their charge with both He and X atoms but X^+ ions could participate only in the symmetric process (20), the values of Q_{HE} and Q_X to be used in the Monte Carlo procedure (equation (6)) are:

$$Q_{HE}(\varepsilon) = n_{HE}\sigma_{HE-HE}(\varepsilon) + n_X\sigma_{HE-X}, \tag{22}$$

$$Q_X(\varepsilon) = n_X\sigma_{X-X}(\varepsilon), \tag{23}$$

where n_{HE} and n_X are the concentrations of He and X atoms, $\sigma_{HE-HE}(\varepsilon)$ and $\sigma_{X-X}(\varepsilon)$ are the cross sections of symmetric processes (19) and (20) and σ_{HE-X} is the cross section of the asymmetric process (21). The cross sections of the symmetric processes depend weakly on the v^+ ion velocity and are given by the Firsov formula (Firsov 1951, Rapp and Francis 1962, Sinha and Bardsley 1976):

$$\sigma_s^{1/2} = a - b\ Ln(v^+). \tag{24}$$

The coefficients a and b were determined from experimental data (Rapp and Francis 1962). The cross section σ_{HE-X} is taken to be independent of the ion energy (Nakai *et al* 1984).

The positions and types of collisions are determined on the basis of random numbers. Null-collision technique is applied as well to increase the speed of calculation. The ions created in charge transfer processes are supposed to start toward the cathode having thermal energy.

We note that in the case of pure He discharge because of the short mean free path of the symmetric charge transfer process (19) the ions may in a first approximation be treated as being in local field equilibrium (Lawler 1985, Den Hartog *et al* 1988).

2.6. The simulation process

The simulation process applied in our model consists of the following steps:

1. Specification of the input parameters: the discharge voltage, partial pressures of admixed gases, the length of the CDS and the number of electrons to be emitted from the cathode.
2. Emission of one electron from the cathode.
3. Tracing the given electron until it reaches the CDS-NG boundary. The secondary electrons and positive ions created in (electron impact and Penning) ionization processes are stored in lists, with their initial parameters (position, magnitude and direction of velocity).
4. If the electron list is not empty take one electron from the list and proceed with 3.
5. Take the ions one-by-one from the He and X ion lists and trace them as they participate in charge transfer processes until they reach the cathode. (No ions diffuse into the CDS from the negative glow.)
6. Repeat from 2 if not all the electrons are emitted yet.

The simulation is usually carried out for few thousand electrons emitted from the cathode. The data accumulated during the run of the simulation provide the base of the calculation of the discharge parameters as shown in the next section.

2.7. Determination of the discharge parameters

In this section first the method for the determination of the length of the CDS is presented and after this the calculation of the other discharge parameters is described. The CDS is divided into a number of intervals having a length of Δx. The discharge parameters which show spatial variation are calculated at each x_i plane (mesh planes). The equations are written using the continuous variable x, but it is recognized that the values of the parameters are known only at the mesh planes.

The length of the CDS is determined iteratively. In the first step of the iteration the simulation described in § 2.6 is

carried out using an approximate initial value of d. Considering the more general case of gas mixtures, as a result of the simulation we obtain the average number of He^+ and X^+ ions arriving to the cathode per emitted electron. Let these numbers be denoted by N^+_{HE} and N^+_X. According to our approximation that electron emission from the cathode occurs only due to positive ion impact, the N^+_{HE} and N^+_X ions should be just enough to liberate a new electron from the cathode i.e. the following equation has to be satisfied:

$$N^+_{HE} \cdot \gamma_{HE} + N^+_X \cdot \gamma_X = 1, \qquad (25)$$

where γ_{HE} and γ_X are the secondary electron emission coefficients for He^+ and X^+ ions. Using the values of N^+_{HE} and N^+_X obtained from the simulation this equation usually does not hold exactly. The values of N^+_{HE} and N^+_X, however, depend on the length of the CDS and in this way d may be increased or decreased if the value of $N^+_{HE} \cdot \gamma_{HE} + N^+_X \cdot \gamma_X$ is less or greater that unity. Then the next step of the iteration is carried out using the modified value of d. This cycle (modification of d and run the simulation again) is repeated until we obtain a value of d which results sufficient number of ions satisfying the equation (25) with a certainty of a few percent. This deviation is allowed because of the "noise" (statistical error) of the Monte Carlo simulation. Having found the approximately correct value of d, the simulation is carried out once again and the other parameters are calculated from the data of this last simulation run.

The secondary electron emission coefficient for positive ion impact was calculated by the following empirical expression (Thum 1979):

$$\gamma_i = 0.0255 \, (0.8 \cdot E_i - 2 \cdot \varphi)^{1.08}, \qquad (26)$$

where E_i and φ (both given in units of eV) are the ionization potential of the gas atom and the work function of the cathode material, respectively. The calculations were carried out

supposing Al cathode (φ=4.26 eV (Michaelson 1977)).

During the MC simulation, as the electrons passing through the CDS the electron energy distribution function (EEDF) builds up at each x_i plane. Since the ions are also traced by MC simulation their energy distribution (IEDF) may be obtained at each x_i plane, as well. The latter is, however, averaged at the mesh planes to obtain the $\langle v^+(x) \rangle$ average ion velocity except at the x=0 plane (i.e. the cathode surface) where the detailed IEDF is also calculated.

The MC simulation of electrons and positive ions also offers the possibility to obtain the average number flux of electrons and ions per one emitted electron at the mesh planes. These quantities are denoted by $F^-(x)$ and $F^+(x)$. Since the electron and ion current densities are related as:

$$j^-(x)/j^+(x) = F^-(x)/F^+(x) \tag{27}$$

and in a stationary discharge the j current density is constant:

$$j = j^-(x) + j^+(x) \tag{28}$$

we find the current density ratios:

$$j^-(x)/j = F^-(x) \; / \; [F^-(x)+F^+(x)], \tag{29a}$$

and

$$j^+(x)/j = F^+(x) \; / \; [F^-(x)+F^+(x)]. \tag{29b}$$

In the case of gas mixtures $F^+(x)$ has the form $F^+(x) = F_A^+(x) + F_B^+(x)$, where the A and B subscripts refer to the parent and the admixed gas. The different current density ratios are given by:

$$j^-(x)/j = F^-(x) \; / \; [F^-(x)+F_A^+(x)+F_B^+(x)], \tag{30a}$$

$$j_A^+(x)/j = F_A^+(x) \; / \; [F^-(x)+F_A^+(x)+F_B^+(x)], \tag{30b}$$

$$j_B^+(x)/j = F_B^+(x) \; / \; [F^-(x)+F_A^+(x)+F_B^+(x)]. \tag{30c}$$

The j total discharge current density may be found in the following way: since $j^-(x)=\rho^-(x)\langle v^-(x)\rangle$ and $j^+(x)=\rho^+(x)\langle v^+(x)\rangle$, where $\langle v^-(x)\rangle$ is the average velocity of electrons obtained from the EEDF, the Poisson equation reads:

$$\frac{dE(x)}{dx} = (1/\varepsilon_0)\; j \left\{ \frac{j^-(x)}{j} \frac{1}{\langle v^-(x)\rangle} - \frac{j^+(x)}{j} \frac{1}{\langle v^+(x)\rangle} \right\} =$$

$$= (1/\varepsilon_0)\; j\; A_1(x) \qquad (31)$$

and similarly in the case of mixtures having a bit more complicated $A_2(x)$ on the rhs of equation (31). Using the $E(x=d)=0$ boundary condition $E(x)$ can be obtained by integrating (31) and the discharge voltage is given by:

$$V = j \cdot (1/\varepsilon_0) \int_{x=0}^{x=d} \int_{\xi=d}^{\xi=x} A_{1,2}(\xi)\; d\xi\; dx. \qquad (32)$$

It is emphasized, that this equation does not mean a linear relation between V and j since the results of the MC simulation at given V are included in $A_{1,2}(\xi)$, it rather provides a possibility to determine j from the results of the simulation. The integration in (32) is carried out numerically since the values of A_1 or A_2 are known on the x_i planes. Using this method the current density corresponding to given voltage can be found, and by running the simulation for different values of V the current density-voltage characteristics of the discharge may be obtained.

3. RESULTS

In this chapter the results of the model for several discharge parameters are presented emphasizing the effects caused by small amounts of admixtures.

In figures showing spatial variation of discharge parameters the position in the CDS is given in relative units. Since the

CDS-NG boundary must be excluded from the simulation because of the zero electric field at this point (see Boeuf and Marode 1982), $x=0$ and $x=1$ correspond to the position of the cathode and to $0.99 \cdot d$, respectively. The contribution of the Penning ionization was calculated in the simulation using an electrode radius of r=4 mm, which is the same as used in our earlier experimental investigations (Donkó *et al* 1991).

3.1. Electron and ion energy distribution functions

The energy distribution of the electrons entering the negative glow (NG) is important from the viewpoint of the applications. Since considerable part of the ionization in the NG is believed to be caused be the high energy electrons (beam electrons) "injected" from the CDS, the high energy part of the EEDF is of particular importance. Beside ionizing the gas the high energy electrons can efficiently excite high-lying atomic energy levels, e.g. produce population inversion in hollow cathode lasers.

The EEDF obtained from the model close to the CDS-NG boundary is shown in figure 2 for a discharge in pure He, at V=300 V, p=5 mbar, d=0.33 cm. As it can be seen the EEDF function has a "tail" representing the high energy electrons. The peak around the electron energy corresponding to the cathode fall voltage (300 V) shows the electrons which did not suffer energy loss in the CDS. The shape of the peak is identical to the initial energy distribution of the electrons emitted from the cathode.

Keeping the discharge voltage (V=300 V) and the total pressure (p=5mbar) constant and mixing as little, as 0.4% of Ar to the parent gas we obtain the EEDF shown in figure 3. As it can be seen the tail of the EEDF is significantly reduced compared to the case of pure He discharge. This means that the number of the high energy electrons is much less even at this very small Ar partial pressure. Slightly stronger reduction of

the number of high energy electrons was obtained in the case of He+Kr and He+Xe mixtures. Ne was found to cause no significant reduction of the high energy tail of the EEDF.

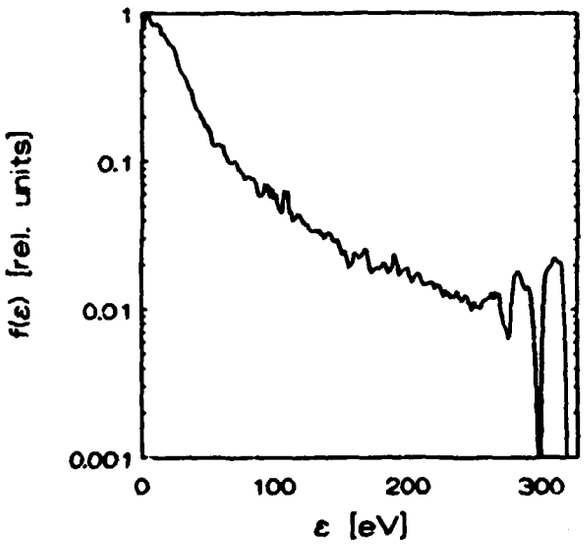

Figure 2.

The EEDF close to the CDS-NG boundary in pure helium discharge at V=300 V.

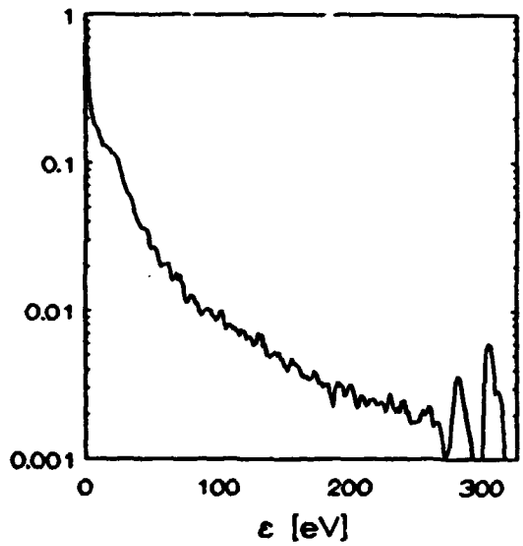

Figure 3.

The EEDF close to the CDS-NG boundary in He + 0.4 % Ar discharge at V=300V.

The $f(\varepsilon^+)$ ion energy distribution (IEDF) on the surface of the cathode is of practical interest, because this determines the sputtering of the cathode material. Figure 4 shows the IEDF at the cathode surface in the case of He+2%Kr mixture. The parameters of the simulation were: V=300 V, p=5 mbar. The energy of He^+ ions has an average value of ≈7 eV and is mostly less than 30 eV. However, the energy distribution of Kr^+ ions (thanks to the "long" mean free path of Kr^+ ions) extends up to the energy corresponding to the maximal available accelerating voltage. The functions shown in figure 4 do not express the ratio of the average number of He^+ and X^+ ions arriving at the cathode, they are normalized as $\int f(\varepsilon^+)d\varepsilon^+=1$.

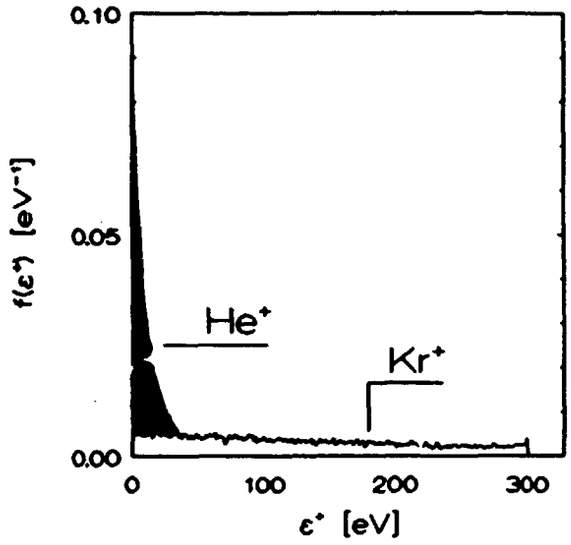

Figure 4.

The energy distribution of He^+ and Kr^+ ions at the cathode surface in He+2%Kr gas mixture (V=300 V).

It can be deduced from figure 4 that in pure He discharge practically no cathode sputtering occurs. Little amounts of admixtures, however, in accordance with experimental observations, may cause significant cathode sputtering (Csillag *et al* 1974). Same amounts of the other admixtures (Ne, Ar and Xe) resulted similar ion energy distribution at the cathode.

3.2. The distribution of the current density

In this section some examples of the current density ratios are given. Figure 5 shows the j^-/j and j^+/j quantities in the CDS in pure He discharge at V=300V and p=5 mbar. The He^+ ions carry about ~3/4 part of the current at the cathode ($x=0$). This is the consequence of the secondary electron emission coefficient being 0.35 as calculated from (26). The share of the electron current increases with x because of the multiplication of the electrons due to ionization processes.

In gas mixtures the ion current is shared between He^+ ions and X^+ ions. As it is illustrated in figure 6 the ions of the low concentration admixed gas (X) carry considerable part of the

low concentration admixed gas (X) carry considerable part of the ion current density. The results are shown for He+0.4%Ar mixture at V=300 V discharge voltage. In this case the Ar^+ ions carry about one third of the ion current density although the Ar concentration is only 1/250 part of the total concentration. Since both He^+ and Ar^+ ions liberate electrons from the cathode and the secondary electron emission of Ar is less than that of He, the ratio of the electron to ion current density slightly decreased at the cathode compared to the case of pure He.

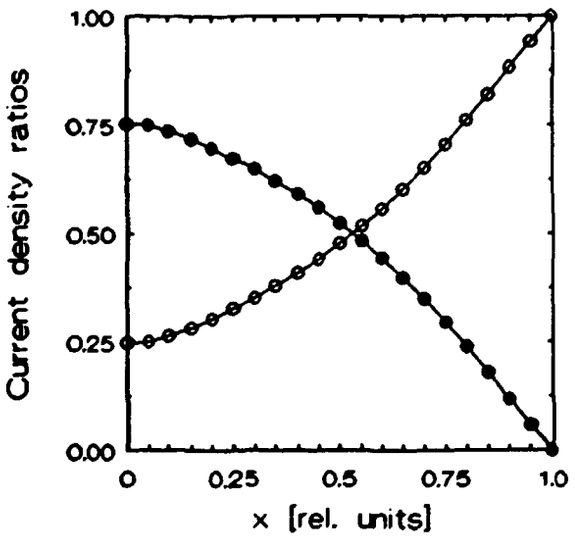

Figure 5.

The distribution of the current density ratios in the CDS in He+0.4%Ar discharge: o *electrons,* • He^+ *ions.*

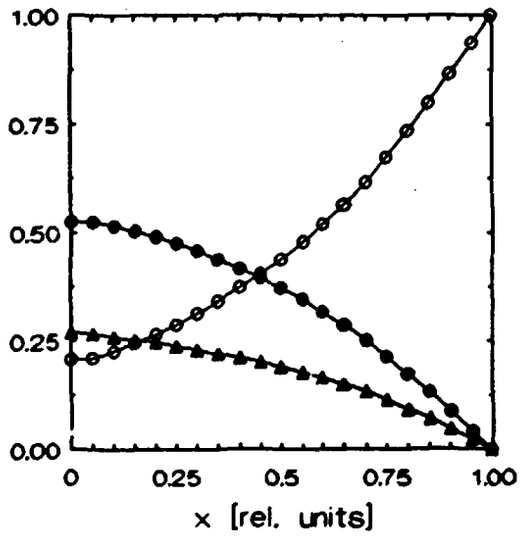

Figure 6.

The distribution of the current density ratios in the CDS in He+0.4%Ar discharge: o *electrons,* • He^+ *ions,* ▲ Ar^+ *ions.*

We found that in the case of Kr and Xe admixtures similarly a significant part of the ion current is taken by the ions of the admixed gas but in He+Ne mixture Ne^+ ions carry negligible part of the ion current. This can be explained by the relatively small ionization cross section of Ne compared to Ar, Kr or Xe

and the absence of the Penning ionization as an ionization source.

3.3. Ionization in the CDS

The α/p reduced ionization coefficient expresses the number of ion pairs created per emitted electron on unit length and at unity pressure.

The spatial dependence of the α/p reduced ionization coefficient in the CDS obtained from the model is plotted in figure 7 for pure He and for He+0.4%Ar mixture. The total gas pressure in both cases was 5 mbar and the voltage was 300 V. It can be seen in figure 7 that 0.4% Ar results an increase of α/p by ≈30% depending on the position x. This enhancement of the ionization is caused by the much higher ionization cross section and the lower ionization potential of Ar compared to He.

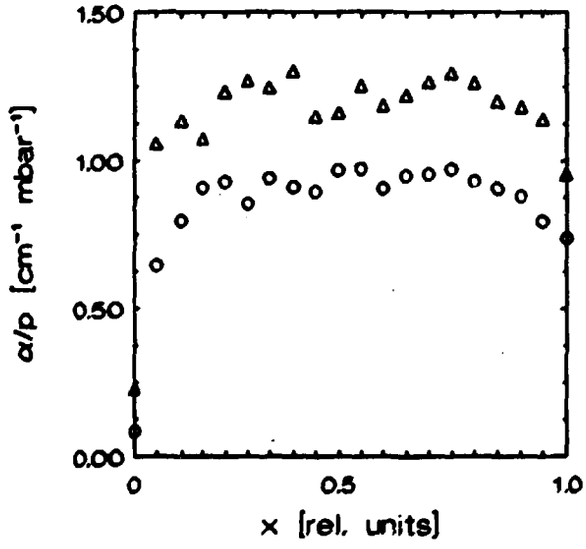

Figure 7.

The α/p reduced ionization coefficient in the CDS in the case of pure He (o) and He+0.4%Ar (Δ) discharges.

It is to be noted that α/p does not vary very much with the position in the CDS except in the vicinity of the cathode ($x \approx 0$). This is the reason why calculations based on average values of

α/p used in the early models of the CDS gave more or less reasonable results.

Similar and a little greater enhancement was obtained in the case of He+Kr and He+Xe mixtures. Admixtures of Ne were found to have no remarkable effect on the α/p ionization coefficient.

3.4. Current density-voltage characteristics

In this section the current density-voltage [$j(V)$] and current density-admixed gas pressure [$j(p_x)$] characteristics obtained from the model are presented and compared to our experimental results (Donkó *et al* 1991).

The calculated and measured $j(V)$ characteristics for pure He discharge in the voltage range of 200-400 V are shown in figure 8. A good agreement between the calculated and measured characteristics can be seen in the whole voltage range.

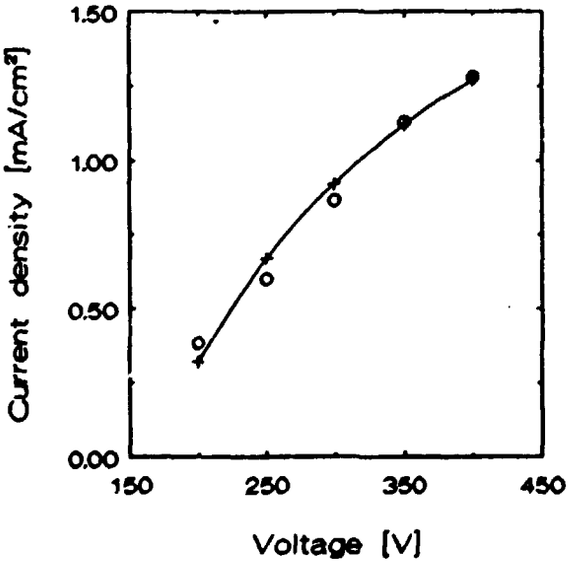

Figure 8.

Measured (+) and calculated (o) current density-voltage [$j(V)$] characteristics of the pure helium discharge (p=5 mbar).

The measured $j(V)$ characteristics of He+0.8%X discharges are shown in figure 9. As it can be seen, 0.8% of Ar admixed to He increases the current density of the discharge by about 20-30% depending on the voltage. The same amount of Xe, however,

decreases j by about 60% in the whole voltage range. In the case of Ne and Kr admixtures a smaller, but definite decrease of the current density was found.

Using the model of the CDS the $j(V)$ characteristics were calculated for the same gas mixture discharges and are presented in figure 10. The results of the model correctly reflect the effect of the admixtures on the current density in the most significant cases, i.e. when Ar or Xe was admixed to He. They do not clearly show the small decrease of j in He+Ne and He+Kr mixtures but they indicate that the current density is not changed very much.

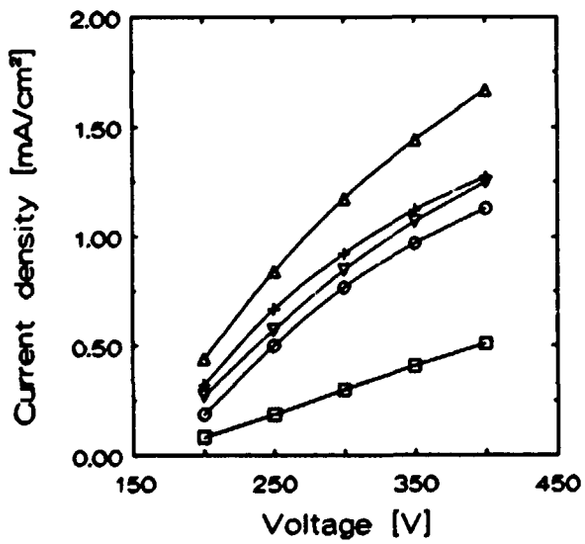

Figure 9.

Measured current density-voltage characteristics of pure He and He + 0.8%X discharges: + He, ○ He+Ne, △ He+Ar, ▽ He+Kr, □ He+Xe.

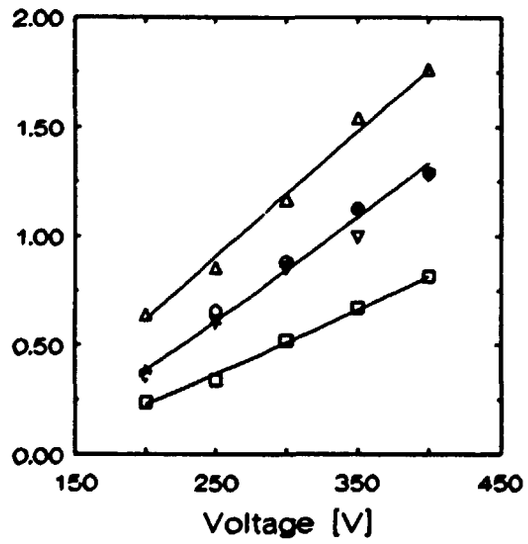

Figure 10.

Calculated current density-voltage characteristics of pure He and He + 0.8%X discharges: + He, ○ He+Ne, △ He+Ar, ▽ He+Kr, □ He+Xe.

The correspondence of the measured and calculated data shows that the changes of the $j(V)$ characteristics can be explained at least qualitatively based on the selected elementary processes.

Let us consider now the most significant cases of Ar and Xe admixtures.

The results of the model indicate that in the case of Xe admixture due to the high cross section of the asymmetric charge transfer process ($\sigma_{HE-XE} \approx 1.5 \times 10^{-15} cm^2$) many of the He^+ ions are lost before they could reach the cathode (more than 50% at 2% Kr concentration) and could induce electron emission. Although there is a considerable additional electron impact and Penning ionization of Xe atoms, but due to the low value of the secondary electron emission coefficient for Xe^+ ions ($\gamma_{XE}=0.03$) the losses of He^+ ions dominate over this additional ionization and this results in a decrease of the current density at constant voltage. According to the results of the model the length of the CDS decreases by about 10% at 0.4% Xe admixture compared to d=0.33 cm in pure He, and it reaches 0.33 cm again as the Xe concentration increases to 2% at V=300 V. We note that while in a pure He discharge the ratio of the electron to the ion current density (i.e. the current balance at the cathode) j^-/j^+ is about 0.35, in the He+2%Xe mixture we obtained $j^-/j^+ \approx 0.1$ (i.e. there are 10 ions needed in average to liberate one electron instead of about 3, as in the case of pure He).

On the other hand, in He+Ar mixtures, the asymmetric charge transfer process (21) has a cross section only $2.7 \times 10^{-16} cm^2$ (less than 1/5 of those of Xe) and the secondary electron emission coefficient for Ar^+ ions is $\gamma_{AR} \approx 0.12$. This means that the He^+ ions are lost with a little probability (less than 10% at 2% Ar concentration) and the Ar^+ ions created by electron impact and Penning ionization processes or in the asymmetric charge transfer process are more likely to induce secondary emission from the cathode (4 times likely compared to Xe^+ ions). These processes lead to the increase of the current density at constant voltage. In He+Ar mixtures the length of the CDS (d) was found to decrease continuously with increasing Ar partial pressure reaching a value of $d \approx 0.25$ cm at 2% Ar concentration (d

was 0.33 cm in pure He discharge at V=300 V). The current balance at the cathode was found to decrease to $j^-/j^+ \approx 0.23$ at 2% Ar admixture.

The Ne and Kr admixtures represent intermediate cases between the two above cases (Xe and Ar) and the current density was found to change in both directions as the p_x partial pressure of the admixtures was changed.

The measured discharge current density as a function of p_x is shown in figure 11. The characteristics are plotted for the different admixtures in the p_x =0-0.1 mbar interval at V=300 V discharge voltage. In the case of Ar admixture j increases monotonly in the whole p_x interval. A continuously decreasing j was observed in He+Xe mixture as the partial pressure of Xe was increased. Ne and Kr admixtures resulted in a little drop of the current density at very low values of p_x (0.01-0.02 mbar) and then j increased slightly with increasing p_x.

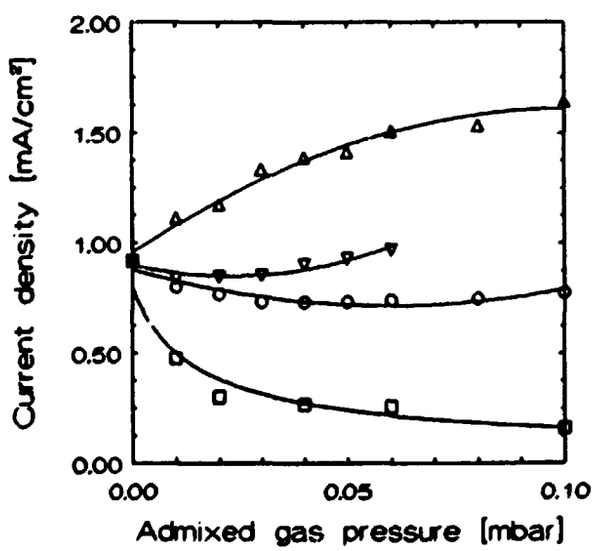

Figure 11.

Measured current density-admixed gas pressure characteristics of He+X discharges:
o He+Ne, Δ He+Ar,
∇ He+Kr, □ He+Xe.
(p=5 mbar, V=300 V)

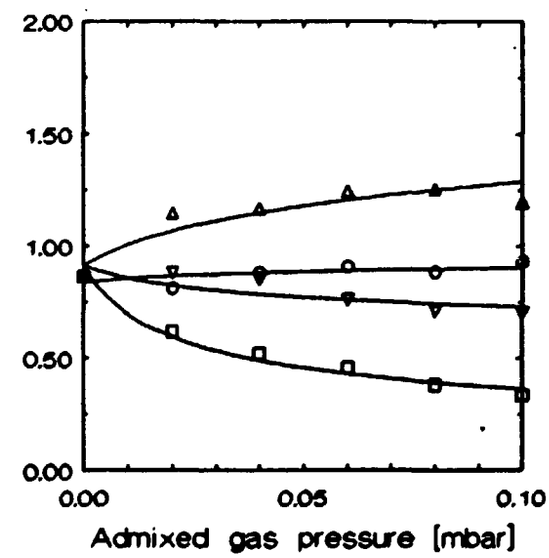

Figure 12.

Calculated current density-admixed gas pressure characteristics of He+X discharges:
o He+Ne, Δ He+Ar,
∇ He+Kr, □ He+Xe.
(p=5 mbar, V=300 V)

The results of our model calculations are plotted in figure 12. There is a reasonable qualitative agreement between the measured and calculated $j(p_x)$ characteristics in the case of He+Ar, He+Ne and He+Xe mixtures The increase of j in He+Ar mixture, as well, as the decrease of j in He+Xe mixture can be clearly seen and the results of the model also reproduce the experimentally observed fact that Ne does not modify remarkably the current density of the discharge. There is a deviation between the measured and calculated figures in He+Kr mixture, where the model fails to predict the experimentally observed small increase of j at Kr partial pressures higher than $\approx$0.03 mbar. The reason of this discrepancy is not yet understood.

3.5. The effect of the admixture on the maintenance of the discharge

One of the simplifying assumptions of the model was that electron emission from the cathode occurs only due to positive ion impact. This condition was formulated in eq. (25). In gas mixtures both He^+ and X^+ ion arrive at the cathode and participate in the maintenance of the discharge. Figure 13 shows the $R=N_x^+ \cdot \gamma_x \cdot 100\%$ quantity as a function of the admixed gas pressure. This quantity expresses the percentage of electrons which are emitted due to the impact of X^+ ions.

It can be seen in figure 13 that the admixtures play an important role in the maintenance of the discharge. In the case of 2% Ar, Kr and Xe admixtures $\sim$25% and in the case of He+2% Ne mixture $\sim$10% of the electrons is emitted from the cathode due to the impact of admixture ions.

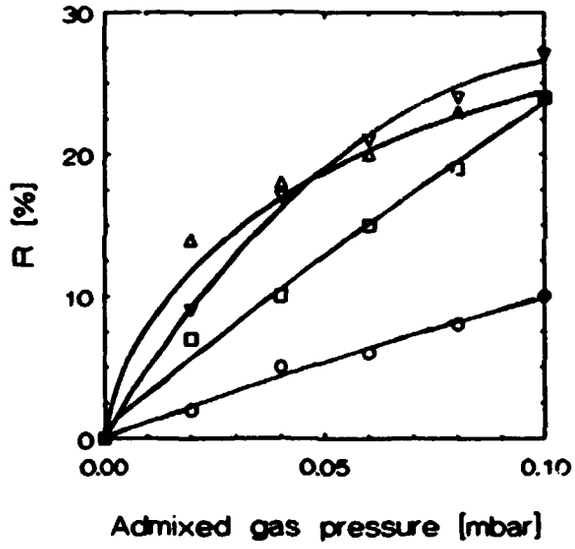

Figure 13.

The percentage of electrons emitted from the cathode due to the impact of admixture ions as functions of the admixed gas pressure.

o Ne^+ *ions,* Δ Ar^+ *ions,*
∇ Kr^+ *ions,* □ Xe^+ *ions.*

3.6. Electric field distribution

Finally we present the electric field distribution obtained from the model to justify our assumption of the linearly decreasing field in the CDS. Figure 14 shows $E(x)$ as it was calculated by the integration of the Poisson equation (31) after calculating the total current density as described in § 2.7. As it can be seen in figure 14, the agreement between the imposed and the calculated field is very good.

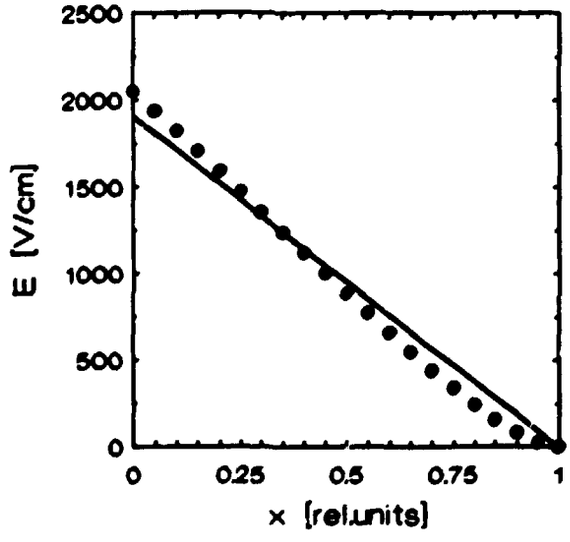

Figure 14.

Specified (———) and calculated (●) electric field distribution in the CDS in pure He discharge (p=5 mbar, V= 300V).

4. CONCLUSIONS

A model of the cathode dark space (CDS) of low current density DC glow discharges was developed. The model applies Monte Carlo treatment of the charged particles and could be used to calculate several discharge parameters (electron and ion energy distribution functions, current density ratios of different charged species, the α/p ionization coefficient, current density - voltage characteristics). Because of the lack of experimental data on the length of the CDS, it was determined in an iterative way, based on the self-maintenance criteria of the discharge.

The aim of this work was primarily to study the changes of the discharge parameters caused by small amounts of admixtures. Helium was used as parent gas and up to 2% of neon, argon, krypton and xenon were used as admixtures.

The electron energy distribution function (EEDF) was found to be strongly affected by the small amounts of admixtures. The high energy part of the EEDF close to the CDS-NG boundary was significantly reduced in the presence of Ar, Kr and Xe. It was observed that a small admixture of Ne does not affect considerably neither the EEDF nor the average velocity of electrons in the CDS. The latter was reduced by about 5, 10 and 20% by 2% admixtures of Ar, Kr and Xe, respectively.

The energy distribution of He^+ and X^+ ions was examined at the cathode surface. The He+ ions were found to have a low average energy at the cathode (≈7 eV at 300 V discharge voltage), what is explained by the short mean free path of He^+ *ions in helium. The energy distribution of the* X^+ *ions (in* all kind of admixtures) was almost uniform in the whole energy interval extending up to the energy corresponding to the cathode fall voltage.

In He+Ar, He+Kr and He+Xe mixtures the current densities carried by He^+ and X^+ ions were comparable even at very low

admixture concentrations. The results of the model indicate that these admixtures have a significant role in the maintenance of the discharge. In 2% mixtures of Ar, Kr or Xe about 25% of the electron emission is caused by the ions of the admixed gas, while the contribution of Ne^+ ions to the electron emission was found to be only 10% in the mixture of He+2%Ne (at a discharge voltage of V=300 V).

The α/p reduced ionization coefficient is considerably enhanced by small amounts of Ar, Kr and Xe admixed to helium (about 30-40% at admixture concentrations of 0.4%). Practically no enhancement of α/p was observed in the case of He+Ne mixtures.

The current density-voltage [$j(V)$] characteristics of the discharge were modified by all admixtures. The changes of the $j(V)$ characteristics were most significant in the case of He+Ar and He+Xe mixtures (Ar was found to increase j and Xe was found to decrease it). The $j(V)$ and $j(p_x)$ characteristics of the gas mixture discharges obtained from the model were compared to experimental data. Good qualitative agreement was found between the two sets of discharge characteristics. The results of the model reproduced the behavior of the $j(V)$ characteristics in all admixtures at 0.8% admixture concentration. The comparison of the $j(p_x)$ characteristics showed a similarly good agreement in the case of Ne, Ar and Xe admixtures in the examined case of V=300 V discharge voltage .

We have found that a considerable part of the primary electrons was produced by the ions of the admixed component even at low admixture concentration.

It was shown that the $E(x)$ electric field distribution obtained from the calculation is very close to our assumption, i.e. to the linearly decreasing electric field in the CDS.

* * *

ACKNOWLEDGMENT:

Discussions on this work with Drs K Rózsa, P Mezei , P Apai and L Csillag are greatfully acknowledged.
We also thank Prof H R Skullerud (The Norwegian Institute of Technology) for his suggestions on the preparation of the manuscript.
This work was partly supported by Hungarian Science Foundation Grant OTKA-F-4475.

REFERENCES:

Boeuf J P and Marode E 1982 *J.Phys.D: Appl.Phys.* 15 2169

Carman R J 1989 *J.Phys.D: Appl.Phys.* 22 55

Chen X, Rózsa K, Chang J S, Seto L, Berezin A A and Kaneda T 1988 *Research Report* DEC.1988/No.36 (Tokyo Denki University)

Csillag L, Jánossy M, Rózsa K and Salamon T 1974 *Phys. Lett.* 50A, 13

Date A, Kitamori K, Sakai Y and Tagashira H 1992 *J.Phys.D: Appl.Phys.* 25 442

Den Hartog E A, Doughty D A and Lawler J E 1988 *Phys.Rev.A* 38 2471

Donkó Z, Rózsa K and Jánossy M 1991 *J.Phys.D: Appl.Phys.* 24 1322

Doughty D A, Den Hartog E A and Lawler J E 1987 *Phys.Rev.Lett.* 58 2668

Firsov O B 1951 *Zh.Eksp.Teor.Fiz.* 21 1001

Graves D B and Surendra M 1990 *Non-Equilibrium Effects in DC and RF Glow Discharges,* in *Nonequilibrium Effects in Ion and Electron Transport* (ed. Gallagher J W, Plenum Press, New York) p.157

Hagstrum H D 1956 *Phys.Rev.* **104** 317

Hashiguchi S and Hasikuni M 1988 *Japanese J.Appl.Phys.* **27** 1010

Hashiguchi S 1991 *IEEE Transactions on Plasma Science* **19** 297

de Heer F J and Jansen R H J 1977 *J.Phys.B: At.Mol.Phys.* **10** 3741

de Heer F J, Jansen R H J and van der Kaay W 1979 *J.Phys.B: At.Mol.Phys.* **12** 979

Helm H 1979 *Beitr.Plasmaphysik* **18** 233

Jianfen Liu and Govinda Raju G R 1992 *J.Phys.D: Appl.Phys.* **25** 167

Kruithof A A and Penning F M 1937 *Physica* **4** 430

Lawler J E 1985 *Phys.Rev.A* **32** 2977

Marode E and Boeuf J P 1983 in *Proceedings of the XVIth International Conference on Phenomena in Ionized Gases* Düsseldorf, *Invited Papers* (ed. Bötticher W, Wenk H and Schulz-Gulde E) p.206

Michaelson H B 1977 *J. Appl. Phys.* **48** 4729

Molnar J P 1951 *Phys.Rev.* **83** 940

Muschlitz E E and Scholette W P 1960 *Report* G-5967 (University. of Florida)

Nakai T, Kikuchi A, Shirai T and Sataka M 1984 *Report* JAERI-M 84-069 (Japan Atomic Energy Research Institute)

Ohuchi M and Kubota T 1983 *J.Phys.D: Appl.Phys.* **16** 1705

Pitchford L C, Boeuf J P, Segur P and Marode E 1990 *Non-Equilibrium Electron Transport: A Brief Overview,* in *Nonequilibrium Effects in Ion and Electron Transport* (ed. Gallagher J W, Plenum Press, New York) p.1

Rapp D and Francis W E 1962 *J.Chem.Phys.* **37** 2631

Rózsa K and Jánossy M 1983 in *Proceedings of the XVIth International Conference on Phenomena in Ionized Gases* Düsseldorf, *Invited Papers* (ed. Bötticher W, Wenk H and Schulz-Gulde E) p.150

Shi B, Fetzer G J, Yu Z, Meyer J D and Collins G J 1989 *IEEE J.Quantum Electronics* QE-25 948

Sinha S and Bardsley J N 1976 *Phys.Rev.A* 14 104

Skullerud H R 1968 *J.Phys.D: Appl.Phys.* 1 1567

Solanki R, Latush E L, Gerstenberger D C, Fairbank W M Jr and Collins G J 1979 *Appl.Phys.Lett.* 35 317

Sommerer T J and Lawler J E 1988 *J.Appl.Phys.* 64 1775

Thum F 1979 *Report* IIP 9/29 (Max Planck Institute for Plasmaphysics)

Tran Ngoc An, Marode E and Johnson P C 1977 *J.Phys.D: Appl.Phys.* 10 2317

Walsh A 1955 *Spectrochim Acta* 7 108

Warren R 1955 *Phys.Rev.* 98 1650

Weston G F 1968 *Cold Cathode Glow Discharge Tubes* (ILIFFE Books, London)

Willett C S 1974 *Introduction to Gas Lasers: Population Inversion Mechanisms* (Pergamon Press)

Yumoto M, Kuroda Y and Sakai T 1991 *J.Phys.D: Appl.Phys.* 24 1594

The issues of the KFKI preprint/report series are classified as follows:

A. Particle and Nuclear Physics
B. General Relativity and Gravitation
C. Cosmic Rays and Space Research
D. Fusion and Plasma Physics
E. Solid State Physics
F. Semiconductor and Bubble Memory Physics and Technology
G. Nuclear Reactor Physics and Technology
H. Laboratory, Biomedical and Nuclear Reactor Electronics
I. Mechanical, Precision Mechanical and Nuclear Engineering
J. Analytical and Physical Chemistry
K. Health Physics
L. Vibration Analysis, CAD, CAM
M. Hardware and Software Development, Computer Applications, Programming
N. Computer Design, CAMAC, Computer Controlled Measurements

The complete series or issues discussing one or more of the subjects can be ordered; institutions are kindly requested to contact the KFKI Library, individuals the authors.

Title and classification of the issues published this year:

KFKI-1992-01/E A. Czitrovszky et al.: Laser analysis of aerosol particles to calculate distribution of aerosol electric charges and size

KFKI-1992-02/A F. Glück et al.: Order-α radiative corrections for semileptonic decays of polarized baryons

KFKI-1992-03/A L. Diósi: Coarse graining and decoherence translated into von Neumann Language

KFKI-1992-04/E L. Diósi: On the Caldeira-Leggett Master Equation

KFKI-1992-05/B+M J. Kadlecsik: Tensor Manipulation Package for General Relativity Calculations

KFKI-1992-06/B G.S. Hall: Symmetries in General Relativity - a brief survey
C. Hoenselaers: Nonlinear Partial Differential Equations and Solitons

KFKI-1992-07/A L.L. Gabunia, T.Gémesy, L. Jenik, A.I. Kharchilava, S. Krasznovszky, V.N. Penev, Gy. Pintér, A.I. Shidovskaja, L.S. Vertogradov: Production region of identical pions at 38 GeV/c p^--nuclei interactions with high P_t particles

KFKI-1992-08/A K. Szlachányi, P. Vecsernyés: Quantum Symmetry and Braid Group Statistics in G-spin Models

KFKI-1992-09/G A. Rácz: Estimation of Quasi-Critical Reactivity

KFKI-1992-10/A+B A. Frenkel and F. Károlyházy: Progress in the K-model of Quantum mechanics

KFKI-1992-11/A J. Révai, Y. Nogami: On the theory of atomic ionization following alpha decay

KFKI-1992-12/A I. Lovas, L. Molnár, K. Sailer, W. Greiner: Periodic structure in nuclear matter

KFKI-1992-13/A S. Krasznovszky: Analysis of the KW Distribution Using a Generalization of the Meijer's G-function

KFKI-1992-14/M Mária Törő: Performance Analysis of the IIASA Network

KFKI-1992-15/A F. Glück: Measurable distributions of unpolarized neutron decay

KFKI-1992-16/J Sz. Török, Sz. Sándor et. all: Source apportionment of individual aerosol particles at Hungarian background stations

KFKI-1992-17/G G. Pór, L. A. Sokolov: "KAZMER" A Complex noise diagnostic system for 1000 MWe PWR WWER Type Nuclear Power Units

KFKI-1992-18/G S. Lipcsei, S. Kiss and G. Pór: On the Eigenfrequencies of Fuel Rod Vibration in NPPs Submitted to Annals of Nuclear Energy

KFKI-1992-19/G,I P. Pellionisz, S.K. Jha and G.L. Goswami: Acoustic Emission Experiments for PHWR Technology Development

KFKI-1992-20/K P. Zombori, A. Andrási, I. Németh: A New Method for the Determination of Radionuclide Distribution in the Soil by In Situ Gamma-Ray Spectrometry

KFKI-1992-21/A L. Diósi: On Digital Randomness of Quantum Coordinates

KFKI-1992-22/B C. Hoenselaers, Z. Perjés: Remarks on the Robinson-Trautman solutions

KFKI-1992-23/G B. Lukács and A. Rácz: Objective Judgement by Kalman Filtering in the Generalized Landsbergian Scheme

KFKI-1992-24/E G. Konczos, B. Selmeci: Amorphous Alloys Bibliography 1987-1991: Papers from the Central Research Institute for Physics (Budapest) and Cooperating Institutions

KFKI-1992-25/G S. Bende-Farkas, S. Kiss and A. Rácz: Logic Based Feature Detection on Incore Neutron Spectra

KFKI-1992-26/G J. Végh, J. Huszár, J. Láz: Development of an X Window based operator's interface for a core monitoring system

KFKI-1992-27/G Vértes P.: Code for Calculation of Spreading of Radioactivity in Reactor Containment Systems (TIBSO code)

KFKI-1992-28/B,G B. Lukács, A. Rácz: Killing Symmetries in Neutron Transport

KFKI-1992-29/D Z. Donkó and M. Jánossy: Modeling the cathode region of noble gas mixture discharges using Monte Carlo simulation

Kiadja a Központi Fizikai Kutató Intézet
Felelős kiadó: Kroó Norbert
Szakmai lektor: Rózsa Károly
Nyelvi lektor: Rózsa Károly
Példányszám: 188
Készült a PROSPERITÁS Kft. nyomdaüzemében
Budapest, 1992. október hó